

Asymmetry in Microlensing-Induced Light Curves

Kohkichi KONNO and Yasufumi KOJIMA

*Department of Physics, Hiroshima University, Higashi-Hiroshima
739-8526, Japan*

Abstract

We discuss distortion in microlensing-induced light curves which are considered to be curves due to single-point-mass lenses at a first glance. As factors of the distortion, we consider close binary and planetary systems, which are the limiting cases of two-point-mass lenses, and the gravitational potential is regarded as the sum of the single point mass and the corrections. In order to quantitatively estimate the asymmetric features of such distorted light curves, we propose a cutoff dependent skewness, and show how to discriminate the similar light curves with it. We also examine as the distortion the general relativistic effect of frame dragging, but the effect coincides with the close binary case in the light curves.

§1. Introduction

Gravitational microlensing¹⁾ is one important probe for studying the nature and distribution of mass in the galaxy. Chang and Refsdal²⁾ and Gott³⁾ suggested that even though multiple images by lensing are unresolved, the time variation of the magnitude of the source can still be detected if the lens moves relative to the source. Such light curves caused by the microlensing can be distinguished from curves of intrinsically variable sources, because the change of magnitude by lensing is achromatic, whereas the colors of intrinsically variable stars change in general. Furthermore, microlensing-induced light curves can be distinguished from magnification by bursts, which are likely to appear in sheer shapes. As is well known, microlensing by a point mass has the time-symmetric light curves, provided that the lens and the source have constant relative transverse velocity. Hence, most events are expected to have almost time-symmetric light curves. If the relative velocity is not constant, then of course time-asymmetric light curves will be detected. Gould⁴⁾ predicted a parallax effect due to the orbital motion of the Earth, and its effect was indeed detected by Alcock et al.⁵⁾ When the time scale of a microlensing event is larger than ~ 100 days, this effect is important. However, if the time scale is of hours to weeks, the parallax effect can be neglected. Then, other factors, such as the non-spherical gravitational potential of the lens, could also produce distortion from the time-symmetric light curves. The effect may be regarded as a higher-order correction to the point-mass lens. The aim of this paper is to evaluate the effect of the intrinsic nature of the lenses, which may slightly distort the light curves. We exclude significantly peculiar light curves, such as double peaks, from which direct information is available without any detailed analyses. We rather restrict our consideration to light curves which are regarded as curves of single-point-mass lenses at a first glance, that is, almost time-symmetric light curves. Since the asymmetric part contains additional information about massive astrophysical compact halo objects (MACHOs), this subject is very important to understanding the nature of MACHOs.

One of the important factors to induce time-asymmetric forms is the binary system of the lensing objects, in which the contribution from both objects to the Newtonian gravitational potential is no longer spherical. The discussion is simplified by considering two-point-mass lenses. In particular, since we consider almost time-symmetric light curves, we hit on two situations: close binary and planetary systems. In a close binary system, the separation distance between the two point masses is much less than the Einstein radius of the total mass, so that the approximated light curve can be described by the total mass and some corrections to it. The detectability of a close binary system has been discussed in detail by Gaudi and Gould¹¹⁾ considering the excess magnification threshold. According to them, the

detectability of close binaries with separation less than ~ 0.2 of the Einstein radius is $\sim 10\%$. Therefore, most close binary lenses with such small separation are missed. We consider the possibility of picking up the discarded asymmetry, by which even below the separation of ~ 0.2 of the Einstein radius the binary nature of the lenses may be detected. In a planetary system, the light curve is expected to be described by the contribution from the larger mass and some corrections from the smaller one. Several authors^{7), 8), 9), 10), 11)} have discussed planetary systems with remarkable deviations from a single lens. However, we are now interested in planetary events which would be missed due to the special configurations of the lensing geometry. Our new proposal may make the detection of such events possible, in addition to the close binary case. Another factor for the time-asymmetric forms is the asymmetry of the lens object itself. The multipole moment of the lens deviates from gravitational potential of the point mass. The gravitational potential due to the quadrupole never vanishes for the two-point-mass case. Therefore, such a correction term in the gravitational potential can be regarded as the limiting case of the binary. Instead, we shall consider general relativistic effects of dragging of inertial frames due to a rotating object as another factor, which cannot be expressed as corrections to the Newton-like potential. While the Newton-like potential corresponds to the gravitoelectric field, this effect results from the gravitomagnetic field. In this case, corrections up to post-Newtonian order are sufficient. Other post-Newtonian potentials also affect the light curves, but they are neglected here.

This paper is organized as follows. In §2 we discuss the two situations involving the two-point-mass lenses and obtain microlensing-induced light curves slightly deviating from the time-symmetric curves. In §3 we discuss the post-Newtonian corrections due to the rotation and obtain time-asymmetric light curves as well. We propose a certain tool to estimate the time-asymmetric features quantitatively in §4. Finally, we give summary and discussion in §5.

§2. Two-point-mass lenses

We investigate two extreme situations involving two-point-mass lenses in order. (The general computational details including critical lines and caustics can be found in Ref. 12).) First, we consider the situation in which the distance l between the two point masses is much less than the Einstein radius r_E corresponding to the total mass. Next, we consider the situation in which one mass, M_1 , is much smaller than the other mass, M_2 .

2.1. Close binary system

We consider the lens plane on to which the positions of the two point masses M_1 and M_2 are projected (see Fig. 1). We introduce an angular coordinate system (θ_x, θ_y) , in which the two point masses lie on the θ_x -axis and the origin is chosen as their geometrical center. We also define an angular coordinate system (β_x, β_y) in the source plane, corresponding to the lens plane. We express the distance between the observer and the lens plane, the lens plane and the source plane, and the observer and the source plane by D_L , D_{LS} and D_S , respectively.

If we denote the angular separation between the source and the image by α , we have

$$\alpha_x = \frac{4GM_1}{c^2} \frac{D_{LS}}{D_L D_S} \frac{\theta_x - \eta}{(\theta_x - \eta)^2 + \theta_y^2} + \frac{4GM_2}{c^2} \frac{D_{LS}}{D_L D_S} \frac{\theta_x + \eta}{(\theta_x + \eta)^2 + \theta_y^2}, \quad (2.1a)$$

$$\alpha_y = \frac{4GM_1}{c^2} \frac{D_{LS}}{D_L D_S} \frac{\theta_y}{(\theta_x - \eta)^2 + \theta_y^2} + \frac{4GM_2}{c^2} \frac{D_{LS}}{D_L D_S} \frac{\theta_y}{(\theta_x + \eta)^2 + \theta_y^2}, \quad (2.1b)$$

where η is the angular separation of the mass M_1 (or M_2) from the optical axis. Therefore, the lens equation can be written in the form

$$\beta = \theta - \alpha. \quad (2.2)$$

We normalize this equation by the Einstein radius for the total mass,

$$\theta_E = \left(\frac{4G(M_1 + M_2)}{c^2} \frac{D_{LS}}{D_L D_S} \right)^{\frac{1}{2}}, \quad (2.3)$$

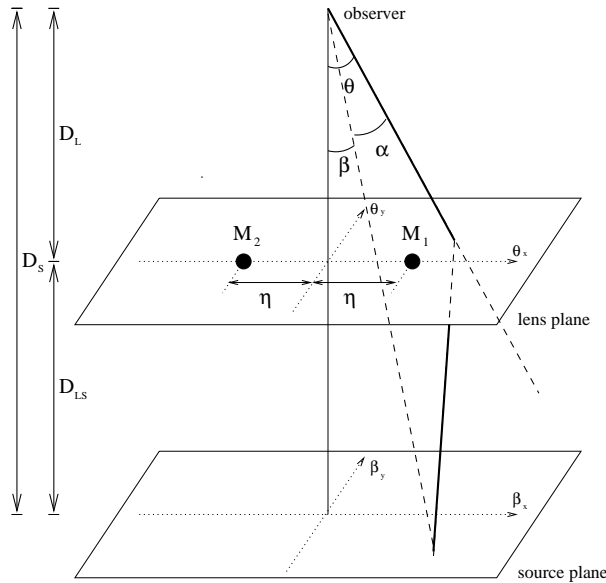


Fig. 1. Geometry of the gravitational lensing considered in §2.1.

and introduce normalized quantities

$$\tilde{\boldsymbol{\beta}} \equiv \frac{\boldsymbol{\beta}}{\theta_E}, \quad \tilde{\boldsymbol{\theta}} \equiv \frac{\boldsymbol{\theta}}{\theta_E}, \quad \tilde{\eta} \equiv \frac{\eta}{\theta_E}. \quad (2.4)$$

The lens equation is then given by

$$\tilde{\beta}_x = \tilde{\theta}_x - \mu_1 \frac{\tilde{\theta}_x - \tilde{\eta}}{(\tilde{\theta}_x - \tilde{\eta})^2 + \tilde{\theta}_y^2} - \mu_2 \frac{\tilde{\theta}_x + \tilde{\eta}}{(\tilde{\theta}_x + \tilde{\eta})^2 + \tilde{\theta}_y^2}, \quad (2.5a)$$

$$\tilde{\beta}_y = \tilde{\theta}_y - \mu_1 \frac{\tilde{\theta}_y}{(\tilde{\theta}_x - \tilde{\eta})^2 + \tilde{\theta}_y^2} - \mu_2 \frac{\tilde{\theta}_y}{(\tilde{\theta}_x + \tilde{\eta})^2 + \tilde{\theta}_y^2}, \quad (2.5b)$$

where μ_1 and μ_2 are defined as

$$\mu_1 = \frac{M_1}{M_1 + M_2}, \quad \mu_2 = \frac{M_2}{M_1 + M_2}. \quad (2.6)$$

The separation distance in the projected plane is $l = D_L \cdot 2\eta$, and the Einstein radius for this system $r_E = D_L \cdot \theta_E$. The term ‘close binary’ in the gravitational lens means $l \ll r_E$. This condition in the astronomical situation is expressed as $l \ll 10^{14}(M/M_\odot)^{1/2} (D/(10 \text{ kpc}))^{1/2} \text{ cm}$, where we have chosen typical astronomical distances as the scale of the galactic halo, $D_{LS} \sim D_L \sim D_S \sim D$. Therefore, the range of applicability is not so severely limited. The condition of the close binary, $l \ll r_E$, is mathematically expressed as

$$\tilde{\eta} \ll 1. \quad (2.7)$$

Under this condition, we expand the right-hand side of the lens equation with respect to $\tilde{\eta}$. Up to first order in $\tilde{\eta}$, we have

$$\tilde{\beta}_x = \tilde{\theta}_x - \frac{\tilde{\theta}_x}{\tilde{\theta}_x^2 + \tilde{\theta}_y^2} - \tilde{\eta}(\mu_1 - \mu_2) \frac{\tilde{\theta}_x^2 - \tilde{\theta}_y^2}{(\tilde{\theta}_x^2 + \tilde{\theta}_y^2)^2}, \quad (2.8a)$$

$$\tilde{\beta}_y = \tilde{\theta}_y - \frac{\tilde{\theta}_y}{\tilde{\theta}_x^2 + \tilde{\theta}_y^2} - \tilde{\eta}(\mu_1 - \mu_2) \frac{2\tilde{\theta}_x\tilde{\theta}_y}{(\tilde{\theta}_x^2 + \tilde{\theta}_y^2)^2}, \quad (2.8b)$$

where the last term on each right-hand side represents the deviation from a single-point-mass lens. The first-order corrections vanish for the equal mass case, since $\mu_1 = \mu_2$. It is therefore convenient to express the combination $\tilde{\eta}(\mu_1 - \mu_2)$ as one small parameter $\varepsilon \equiv \tilde{\eta}(\mu_1 - \mu_2)$.

The inversion of Eq. (2.8), i.e., solving $\tilde{\boldsymbol{\theta}}$ by $\tilde{\boldsymbol{\beta}}$, is possible, but the general form is quite messy. However, under the condition $\varepsilon \ll 1$, the approximate solution, i.e., the first-order solution in ε , is given by the form

$$\tilde{\boldsymbol{\theta}} = \tilde{\boldsymbol{\theta}}_0 + \varepsilon \tilde{\boldsymbol{\theta}}_1, \quad (2.9)$$

where $\tilde{\theta}_0$ and $\tilde{\theta}_1$ denote the zeroth-order and the first-order solutions, respectively. Substituting Eq. (2.9) into Eqs. (2.8), we can find such solutions. The zeroth-order solution is given by

$$\tilde{\theta}_{0x} = \frac{1}{2} \left(\tilde{\beta}_x \pm \tilde{\beta}_x \sqrt{1 + \frac{4}{\tilde{\beta}_x^2 + \tilde{\beta}_y^2}} \right), \quad (2.10a)$$

$$\tilde{\theta}_{0y} = \frac{1}{2} \left(\tilde{\beta}_y \pm \tilde{\beta}_y \sqrt{1 + \frac{4}{\tilde{\beta}_x^2 + \tilde{\beta}_y^2}} \right). \quad (2.10b)$$

Using this zeroth-order solution, the first-order solution is written in the form

$$\tilde{\theta}_{1x} = \frac{\tilde{\theta}_{0x}^2 - \tilde{\theta}_{0y}^2 - 1}{(\tilde{\theta}_{0x}^2 + \tilde{\theta}_{0y}^2)^2 - 1}, \quad (2.11a)$$

$$\tilde{\theta}_{1y} = \frac{2\tilde{\theta}_{0x}\tilde{\theta}_{0y}}{(\tilde{\theta}_{0x}^2 + \tilde{\theta}_{0y}^2)^2 - 1}. \quad (2.11b)$$

Next, we turn our attention to the derivation of magnification. The magnification M is given by

$$\begin{aligned} M &= M_+ + M_- \\ &= \left| \det \left(\frac{\partial \tilde{\beta}_i}{\partial \tilde{\theta}_j} \right)_+ \right|^{-1} + \left| \det \left(\frac{\partial \tilde{\beta}_i}{\partial \tilde{\theta}_j} \right)_- \right|^{-1}, \end{aligned} \quad (2.12)$$

where the subscript (+) and (−) correspond to solutions with a plus sign and with a minus sign, respectively, in Eqs. (2.10). The inverse of the Jacobian $\det \left(\frac{\partial \tilde{\beta}_i}{\partial \tilde{\theta}_j} \right)$ is calculated, up to first order in ε , in the following way:

$$\begin{aligned} \left[\det \left(\frac{\partial \tilde{\beta}_i}{\partial \tilde{\theta}_j} \right) \right]^{-1} &= \left[1 - \frac{1}{(\tilde{\theta}_{0x}^2 + \tilde{\theta}_{0y}^2)^2} - \varepsilon \frac{4\tilde{\theta}_{0x}}{(\tilde{\theta}_{0x}^2 + \tilde{\theta}_{0y}^2)^3} + \varepsilon \frac{4(\tilde{\theta}_{0x}\tilde{\theta}_{1x} + \tilde{\theta}_{0y}\tilde{\theta}_{1y})}{(\tilde{\theta}_{0x}^2 + \tilde{\theta}_{0y}^2)^3} \right]^{-1} \\ &= \left(1 - \frac{1}{(\tilde{\theta}_{0x}^2 + \tilde{\theta}_{0y}^2)^2} \right)^{-1} \left[1 + \varepsilon \frac{4\tilde{\theta}_{0x}}{(\tilde{\theta}_{0x}^2 + \tilde{\theta}_{0y}^2 + 1)^2 (\tilde{\theta}_{0x}^2 + \tilde{\theta}_{0y}^2 - 1)} \right]. \end{aligned} \quad (2.13)$$

Therefore, using Eqs. (2.10), (2.12) and (2.13), we can derive the magnification as a function of the source position:

$$M = M(\beta_x, \beta_y; \varepsilon). \quad (2.14)$$

The time variation is produced by the relative change of the positions. The time variation of the magnitude Δm is then given by

$$\Delta m = \Delta m(t) = 2.5 \log_{10} M(\beta_x(t), \beta_y(t); \varepsilon), \quad (2.15)$$

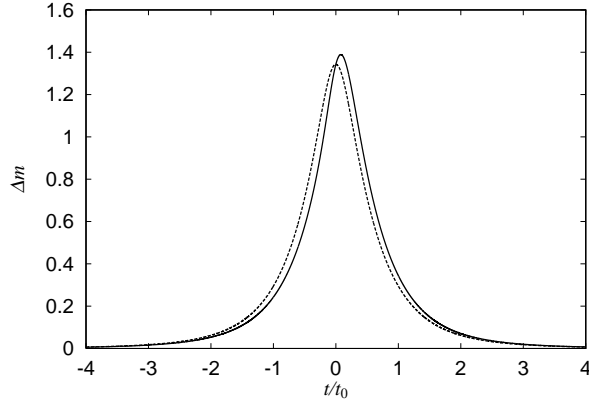


Fig. 2. Microlensing-induced light curves with (solid) and without (dashed) correction for the deviation from a single-point-mass lens. The light curve with the correction is plotted for the small parameter value $\varepsilon = 0.1$. The relative motion of the source to the lens is assumed to be described by $\varphi = 0$ and $p = 0.3$.

where the relative source trajectory is in general described by

$$\tilde{\beta}_x(t) = \frac{t}{t_0} \cos \varphi + p \sin \varphi, \quad (2.16a)$$

$$\tilde{\beta}_y(t) = \frac{t}{t_0} \sin \varphi - p \cos \varphi, \quad (2.16b)$$

where t_0 is the time taken to cross the Einstein radius, φ is the angle of the trajectory from the β_x -axis, and p is the impact parameter normalized by the Einstein radius. From this, we can derive the microlensing-induced light curves, slightly deviating from the time-symmetric curves. An example of the light curves is shown in Fig. 2 for $\varphi = 0$ and $p = 0.3$. The solid line denotes the light curve with the correction for the deviation from a single-point-mass lens, while the dashed line corresponds to the single-point-mass lens. The more general dependence on the angle φ and the impact parameter p is discussed in detail in §4.

2.2. Planetary system

In this subsection, we discuss the case that the mass M_1 is much smaller than M_2 ; that is, the object with smaller mass is regarded as the planet. In this situation, it is convenient to choose the origin of the (θ_x, θ_y) system to be at the position of mass M_2 . Furthermore, let the angular separation between the mass M_1 and M_2 be η (see Fig. 3). Then the normalized lens equation is given by

$$\tilde{\beta}_x = \tilde{\theta}_x - \frac{\tilde{\theta}_x}{\tilde{\theta}_x^2 + \tilde{\theta}_y^2} - \mu \frac{\tilde{\theta}_x - \tilde{\eta}}{(\tilde{\theta}_x - \tilde{\eta})^2 + \tilde{\theta}_y^2}, \quad (2.17a)$$

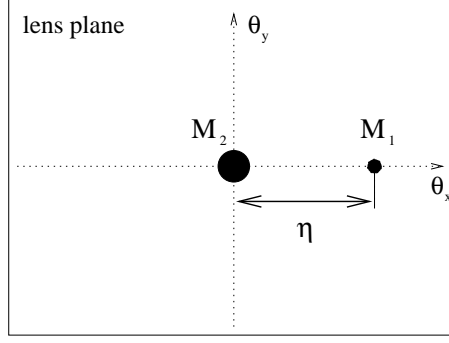


Fig. 3. The lens plane considered in §2.2. The angular separation of the two point masses is denoted by η .

$$\tilde{\beta}_y = \tilde{\theta}_y - \frac{\tilde{\theta}_y}{\tilde{\theta}_x^2 + \tilde{\theta}_y^2} - \mu \frac{\tilde{\theta}_y}{(\tilde{\theta}_x - \tilde{\eta})^2 + \tilde{\theta}_y^2}, \quad (2.17b)$$

where $\mu = M_1/M_2 (\ll 1)$, and we have used for the normalization the Einstein radius of the mass M_2 ,

$$\theta_E = \left(\frac{4GM_2}{c^2} \frac{D_{LS}}{D_L D_S} \right)^{\frac{1}{2}}. \quad (2.18)$$

As in the previous subsection, in the situation $\mu \ll 1$, we approximate the solutions of the lens equation up to first order in μ . Using the zeroth-order solution (2.10), we obtain the first-order solution

$$\tilde{\theta}_{1x} = \frac{\left[(\tilde{\theta}_{0x}^2 + \tilde{\theta}_{0y}^2)^2 - (\tilde{\theta}_{0x}^2 - \tilde{\theta}_{0y}^2) \right] (\tilde{\theta}_{0x} - \tilde{\eta}) - 2\tilde{\theta}_{0x}\tilde{\theta}_{0y}^2}{\left[(\tilde{\theta}_{0x}^2 + \tilde{\theta}_{0y}^2)^2 - 1 \right] \left[(\tilde{\theta}_{0x} - \tilde{\eta})^2 + \tilde{\theta}_{0y}^2 \right]}, \quad (2.19a)$$

$$\tilde{\theta}_{1y} = \frac{\tilde{\theta}_{0y} \left[(\tilde{\theta}_{0x}^2 + \tilde{\theta}_{0y}^2)^2 + (\tilde{\theta}_{0x}^2 - \tilde{\theta}_{0y}^2) - 2\tilde{\theta}_{0x}(\tilde{\theta}_{0x} - \tilde{\eta}) \right]}{\left[(\tilde{\theta}_{0x}^2 + \tilde{\theta}_{0y}^2)^2 - 1 \right] \left[(\tilde{\theta}_{0x} - \tilde{\eta})^2 + \tilde{\theta}_{0y}^2 \right]}. \quad (2.19b)$$

Furthermore, we can calculate the magnification by using Eq. (2.12) and the inverse of the Jacobian $\det \left(\frac{\partial \tilde{\beta}_i}{\partial \tilde{\theta}_j} \right)$, which is up to first order in μ , given by

$$\begin{aligned} \left[\det \left(\frac{\partial \tilde{\beta}_i}{\partial \tilde{\theta}_j} \right) \right]^{-1} &= \left[1 - \frac{1}{(\tilde{\theta}_{0x}^2 + \tilde{\theta}_{0y}^2)^2} + \mu \frac{4(\tilde{\theta}_{0x}\tilde{\theta}_{1x} + \tilde{\theta}_{0y}\tilde{\theta}_{1y})}{(\tilde{\theta}_{0x}^2 + \tilde{\theta}_{0y}^2)^3} \right. \\ &\quad \left. - \mu \frac{2(\tilde{\theta}_{0x}^2 - \tilde{\theta}_{0y}^2) \left[(\tilde{\theta}_{0x} - \tilde{\eta})^2 - \tilde{\theta}_{0y}^2 \right] + 8\tilde{\theta}_{0x}(\tilde{\theta}_{0x} - \tilde{\eta})\tilde{\theta}_{0y}^2}{(\tilde{\theta}_{0x}^2 + \tilde{\theta}_{0y}^2)^2 \left[(\tilde{\theta}_{0x} - \tilde{\eta})^2 + \tilde{\theta}_{0y}^2 \right]^2} \right]^{-1} \\ &= \left(1 - \frac{1}{(\tilde{\theta}_{0x}^2 + \tilde{\theta}_{0y}^2)^2} \right)^{-1} \end{aligned}$$

$$\times \left[1 - \mu \frac{4 (\tilde{\theta}_{0x} \tilde{\theta}_{1x} + \tilde{\theta}_{0y} \tilde{\theta}_{1y})}{(\tilde{\theta}_{0x}^2 + \tilde{\theta}_{0y}^2) [(\tilde{\theta}_{0x}^2 + \tilde{\theta}_{0y}^2)^2 - 1]} + \mu \frac{2 (\tilde{\theta}_{0x}^2 - \tilde{\theta}_{0y}^2) [(\tilde{\theta}_{0x} - \tilde{\eta})^2 - \tilde{\theta}_{0y}^2] + 8 \tilde{\theta}_{0x} (\tilde{\theta}_{0x} - \tilde{\eta}) \tilde{\theta}_{0y}^2}{[(\tilde{\theta}_{0x}^2 + \tilde{\theta}_{0y}^2)^2 - 1] [(\tilde{\theta}_{0x} - \tilde{\eta})^2 + \tilde{\theta}_{0y}^2]^2} \right]. \quad (2.20)$$

Therefore, we can also obtain the microlensing-induced light curves

$$\Delta m = \Delta m(t) = 2.5 \log_{10} M(\beta_x(t), \beta_y(t); \mu), \quad (2.21)$$

where the relative source trajectory is described by Eq. (2.16) using the angle φ and the impact parameter p . Some examples of the light curves with different values of $\tilde{\eta}$ are shown in Fig. 4 for $\mu = 0.05$, $\varphi = 0$ and $p = 0.3$. As seen in these figures, some light curves tend to have double peaks with certain geometrical configurations. The second peak corresponds to the effect of a planet of mass $0.05M_2$. The ratio of the height at the peaks is almost determined by the mass ratio μ . Although we have restricted ourselves to the case $\mu \ll 1$ in order to exclude peculiar light curves, light curves with double peaks are still obtained with certain configurations. This is because the correction term $[(\theta_{0x} - \tilde{\eta}) + \theta_{0y}^2]^{-1}$ becomes effective when θ_{0x} is equal to $\tilde{\eta}$. (More detailed discussions of planetary-binary lensing with dramatic features are given in Refs. 7)–11.)

Furthermore, it is interesting to investigate the configurations in which the Lorentzian curves, i.e., almost time-symmetric light curves arise. For this purpose, we consider the integral of the square of the magnitude difference from the corresponding single-point-mass lens: $\delta \equiv \int_{-\infty}^{+\infty} (\Delta m - \Delta m_0)^2 dt$. The quantity δ indicates the criterion of the deviation from the light curve due to the single-point-mass lens. Figure 5 displays the contours of δ in the $\tilde{\eta}$ - φ space for different impact parameters. Of course, as the quantity δ becomes smaller, the light curve moves closer to that due to the single-point-mass lens. In fact, we can find almost time-symmetric light curves in the domains where δ is smaller than ~ 0.005 , as seen in Fig. 4(b). Such domains tend to become larger as the impact parameter p increases. The same tendency can also be derived by making the mass ratio μ small.

§3. Rotating objects

Several relativistic effects also causes corrections to the point-mass lens. We only consider the dragging effect of inertial frames arising from a rotating object, since other spherical post-Newtonian terms never induce asymmetry in light curves. This additional effect is described

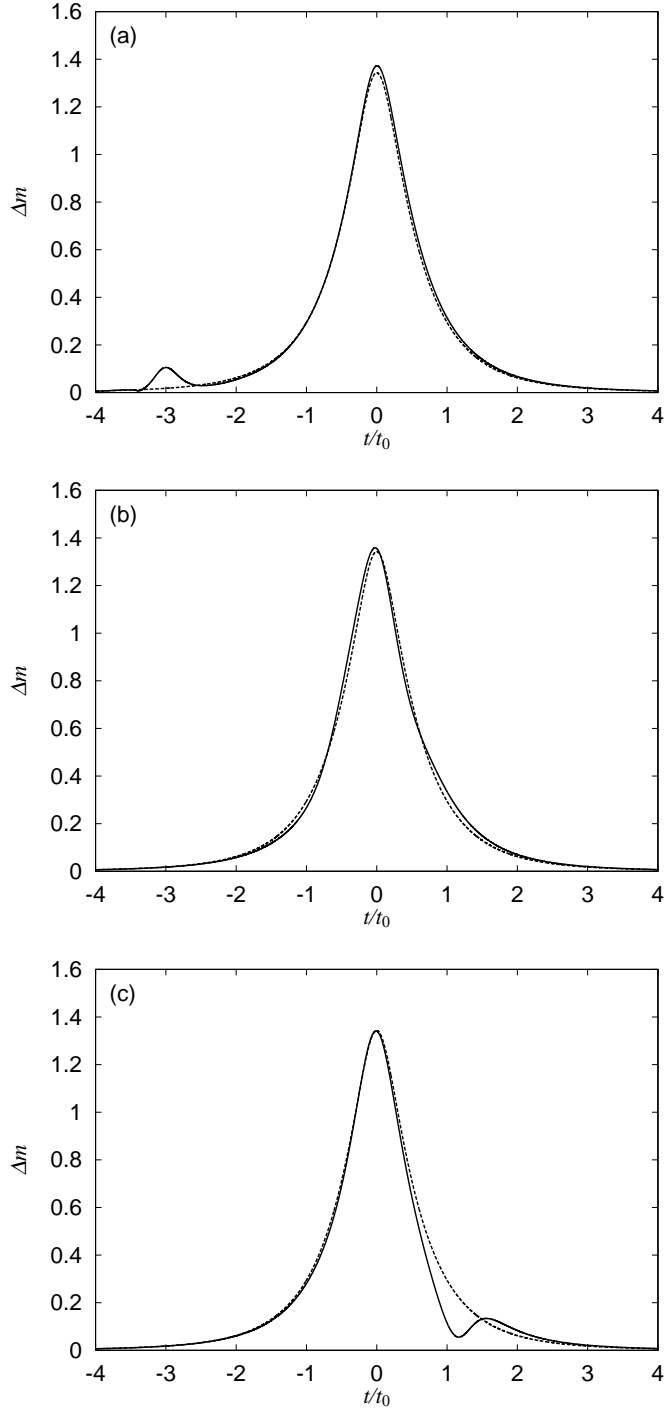


Fig. 4. Microlensing-induced light curves with (solid) and without (dashed) correction for the deviation from a single-point-mass lens. The light curves with the correction are plotted for the case of the small parameter value $\mu = 0.05$ and for angular separations of (a) $\tilde{\eta} = 0.3$, (b) $\tilde{\eta} = 1.0$, and (c) $\tilde{\eta} = 1.7$. The relative motion of the source to the lens is assumed to be described by $\varphi = 0$ and $p = 0.3$.

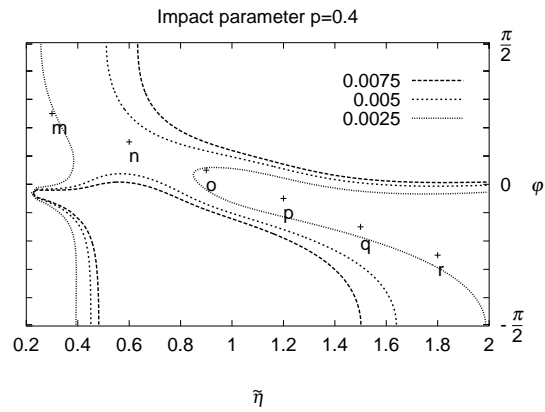
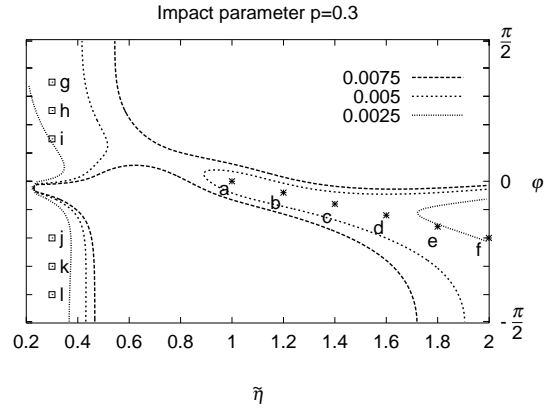
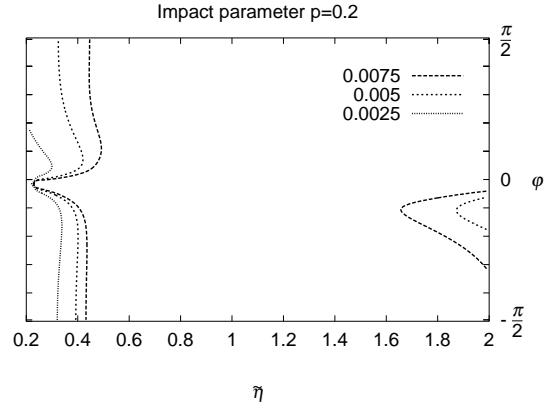


Fig. 5. Contours of δ in $\tilde{\eta}$ - φ space for the impact parameters $p = 0.2, 0.3$ and 0.4 . The small parameter μ is assumed to be 0.05 . The attached labels ‘a’-‘r’ indicate the parameters used in Fig. 10 (see text).

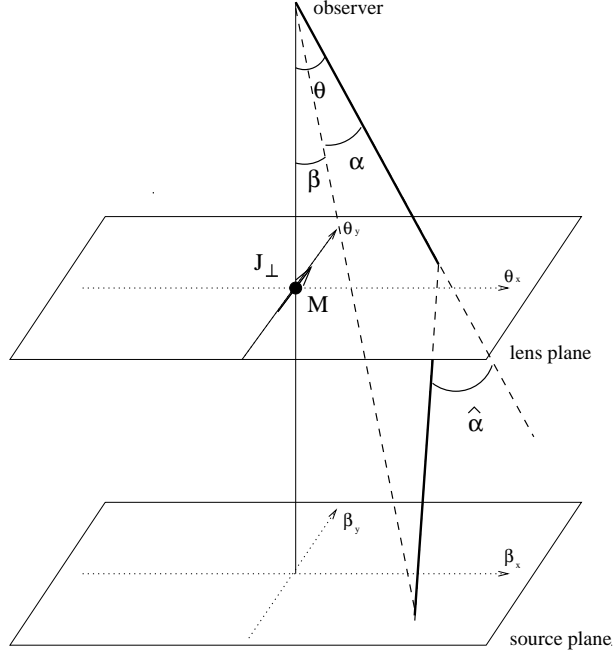


Fig. 6. Geometry of lensing by the rotating object considered in §3.

with the spin angular momentum \mathbf{J} . We consider the projection of the angular momentum of the rotating object on to the lens plane and define the (θ_x, θ_y) coordinate system so that the θ_y -axis is oriented parallel to the projected angular momentum \mathbf{J}_\perp (see Fig. 6). The deflection angles $(\hat{\alpha}_x, \hat{\alpha}_y)$ are written as¹³⁾

$$\hat{\alpha}_x = \frac{4GM}{c^2 D_L} \frac{\theta_x}{\theta_x^2 + \theta_y^2} + \frac{4GJ_\perp}{c^3 D_L^2} \frac{\theta_x^2 - \theta_y^2}{(\theta_x^2 + \theta_y^2)^2}, \quad (3.1a)$$

$$\hat{\alpha}_y = \frac{4GM}{c^2 D_L} \frac{\theta_y}{\theta_x^2 + \theta_y^2} + \frac{4GJ_\perp}{c^3 D_L^2} \frac{2\theta_x \theta_y}{(\theta_x^2 + \theta_y^2)^2}. \quad (3.1b)$$

Hence, we have

$$\alpha_x = \frac{4GM}{c^2} \frac{D_{LS}}{D_L D_S} \frac{\theta_x}{\theta_x^2 + \theta_y^2} + \frac{4GJ_\perp}{c^3} \frac{D_{LS}}{D_L^2 D_S} \frac{\theta_x^2 - \theta_y^2}{(\theta_x^2 + \theta_y^2)^2}, \quad (3.2a)$$

$$\alpha_y = \frac{4GM}{c^2} \frac{D_{LS}}{D_L D_S} \frac{\theta_y}{\theta_x^2 + \theta_y^2} + \frac{4GJ_\perp}{c^3} \frac{D_{LS}}{D_L^2 D_S} \frac{2\theta_x \theta_y}{(\theta_x^2 + \theta_y^2)^2}. \quad (3.2b)$$

Therefore, using the quantities normalized by the Einstein radius, the lens equation becomes

$$\tilde{\beta}_x = \tilde{\theta}_x - \frac{\tilde{\theta}_x}{\tilde{\theta}_x^2 + \tilde{\theta}_y^2} - \gamma \frac{\tilde{\theta}_x^2 - \tilde{\theta}_y^2}{(\tilde{\theta}_x^2 + \tilde{\theta}_y^2)^2}, \quad (3.3a)$$

$$\tilde{\beta}_y = \tilde{\theta}_y - \frac{\tilde{\theta}_y}{\tilde{\theta}_x^2 + \tilde{\theta}_y^2} - \gamma \frac{2\tilde{\theta}_x\tilde{\theta}_y}{(\tilde{\theta}_x^2 + \tilde{\theta}_y^2)^2}, \quad (3.3b)$$

where γ is given by

$$\gamma = \frac{1}{\theta_E} \cdot \frac{J_\perp}{McD_L}. \quad (3.4)$$

It is interesting that this lens equation is the same as that of the two-point-mass lenses for the close binary system, $l \ll r_E$, with the correspondence $\gamma \leftrightarrow \varepsilon$. Hence, the same asymmetric light curves are obtained. Furthermore, it is impossible to distinguish two such corrections. However, the parameter γ is quite small. For example, we consider a Kerr black hole. The angular momentum is $J \sim GM^2/c$, so that we have $\gamma \sim (GMD_S/(c^2D_LD_{LS}))^{1/2} \ll 1$.

§4. Quantitative estimate

In order to estimate the asymmetry in the light curves quantitatively, we now introduce the notion of ‘skewness’ from statistics.¹⁴⁾ In statistics, the skewness for any distribution function $f(t)$ is defined as

$$\text{skewness} = \frac{1}{N} \int_{-\infty}^{\infty} \left(\frac{t - \mu}{\sigma} \right)^3 f(t) dt, \quad (4.1)$$

where N is the normalization factor, μ the mean, and σ the standard deviation. However, there is a problem in utilizing the skewness exactly in this form. To see this, we consider a single-point-mass lens. The light curve is then given by

$$\Delta m = 2.5 \log_{10} \left[\left| \frac{(\tilde{\theta}_{x_+}^2 + \tilde{\theta}_{y_+}^2)^2}{(\tilde{\theta}_{x_+}^2 + \tilde{\theta}_{y_+}^2)^2 - 1} \right| + \left| \frac{(\tilde{\theta}_{x_-}^2 + \tilde{\theta}_{y_-}^2)^2}{(\tilde{\theta}_{x_-}^2 + \tilde{\theta}_{y_-}^2)^2 - 1} \right| \right]. \quad (4.2)$$

If we set $\tilde{\beta}_x = t/t_0$ and $\tilde{\beta}_y = \text{const.}$ and consider the case that the time t approaches infinity, then we have

$$\tilde{\theta}_{x_+} \rightarrow \tilde{\beta}_x = t/t_0 \ (\rightarrow \infty), \quad (4.3a)$$

$$\tilde{\theta}_{y_+} \rightarrow \tilde{\beta}_y = \text{const.}, \quad (4.3b)$$

$$\tilde{\theta}_{x_-} \rightarrow 0, \quad (4.3c)$$

$$\tilde{\theta}_{y_-} \rightarrow 0. \quad (4.3d)$$

It follows that at large t ,

$$\begin{aligned} \Delta m &\simeq 2.5 \log_{10} \left[\left(1 - \frac{1}{t^4} \right)^{-1} \right] \\ &\simeq \frac{2.5}{\ln 10} \cdot \frac{1}{t^4}. \end{aligned} \quad (4.4)$$

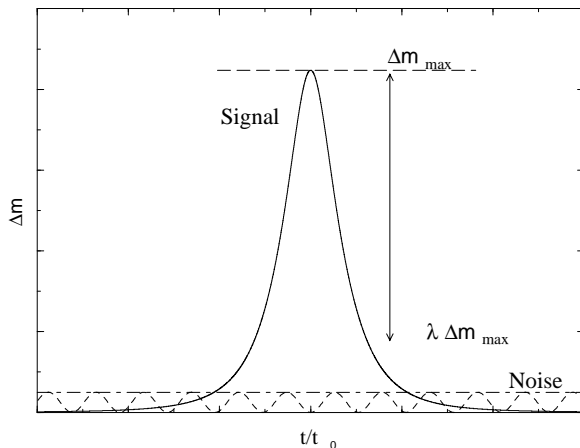


Fig. 7. Illustration of the discussion given in §4. A schematic light curve with noise.

From this, we find that the integral

$$\int_{\mu}^{\infty} t^n \Delta m(t) dt \quad (4.5)$$

diverges if $n \geq 3$. Therefore, we cannot use Eq. (4.1) itself. Nevertheless, since actually observed light curves necessarily include noise, it seems that the integral to infinity is meaningless. With this consideration, we define the skewness for the restricted region of a light curve $\Delta m > \lambda \Delta m_{\max}$, where Δm_{\max} is the maximum value. Here we have introduced the cutoff λ ($0 < \lambda < 1$), and the usual skewness corresponds to $\lambda = 0$. The cutoff will naturally appear in the actual data, e.g., the region $\Delta m < \lambda \Delta m_{\max}$ may be meaningless due to the noise level (see Fig. 7). In microlensing-induced light curves, the bottom level is constant, but the maximum value may have some uncertainty as $(1 \pm \lambda) \Delta m_{\max}$.

We apply this tool to the case of almost identical light curves, which are caused from quite different physical situations, that is, a close binary and a planetary system. The skewness of these light curves are respectively displayed as functions of $1/\lambda$ in Figs. 8–11. Figures 8 and 9 display the dependence of the skewness of the close binary light curves on the angle φ and the impact parameter p , respectively. The light curve given in Fig. 2 corresponds to the curves in Figs. 8 and 9. On the other hand, Figs. 10 and 11 display the skewness of the light curves in the planetary system. In the case of the planetary system, the almost time-symmetric light curves are derived only under certain configurations, as indicated in §2.2. Figure 10 displays the skewness of the light curves under such configurations. The curves labeled by ‘a’–‘r’ correspond to the points labeled by ‘a’–‘r’, respectively, in Fig. 5. Figure 11 displays the impact parameter dependence of the curves corresponding to the point ‘a’. The light curve given in Fig. 4(b) corresponds to the curve ‘a’ in Fig. 10 and a curve in Fig. 11.

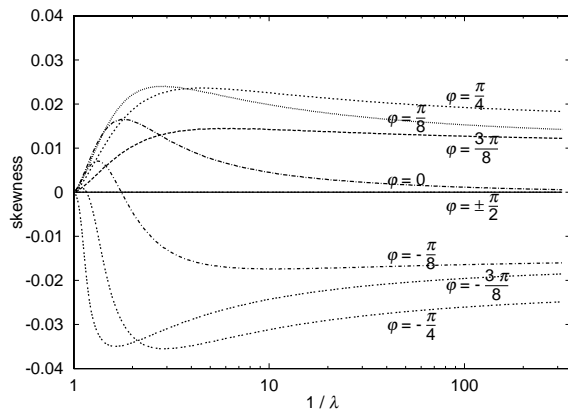


Fig. 8. Dependence of the skewness on the angle φ in the close binary case. The trajectories have the same impact parameter, $p = 0.3$, and the light curves are calculated for the small parameter value $\varepsilon = 0.1$.

As is expected, we have zero skewness when $\varphi = \pm\frac{\pi}{2}$ in Fig. 8. However, when φ is different from $\pm\frac{\pi}{2}$, we have comparable values of the skewness. This demonstrates the useful aspect of the method using the skewness. Nevertheless, the skewness becomes smaller as the impact parameter increases, as seen in Figs. 9 and 11. Thus, the usefulness of the method using the skewness depends mainly on the impact parameter. The skewness with respect to different values of λ fully shows the asymmetric features of the light curves. The absolute values of the skewness depend on the the small parameters ε and μ (i.e., the binary separation and the mass ratio). Furthermore, it should be noted that the absolute values of the skewness have a maximum at $1/\lambda \sim 2-4$ and decrease monotonously in the close binary case, while in the planetary case the skewness indicates different behavior, peaks at larger values of $1/\lambda$, and so on. Therefore, we may discriminate the underlying cases for the asymmetry by the λ -dependent skewness for a good signal-to-noise ratio beyond ~ 10 .

§5. Summary and discussion

We have studied distortion in microlensing-induced light curves which are considered to be curves of single-point-mass lenses at a first glance. In particular, we have attributed factors inducing the distortion to lenses themselves and considered two sorts of corrections: corrections due to deviation from the Newtonian gravitational potential $\phi = -GM/r$ and corrections due to general relativistic effects of dragging of inertial frames arising from a rotating object. For simplicity, we have discussed two extreme cases in two-point-mass lenses for the corrections of the potential; one is the close binary case in which $l \ll r_E$, and the other is the planetary system case in which $M_1 \ll M_2$. Moreover, we have considered

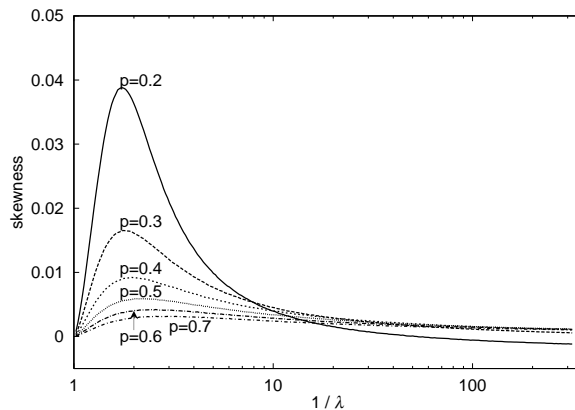


Fig. 9. Dependence of the skewness on the impact parameter p in the close binary case. The trajectories have the same angle, $\varphi = 0$, and the light curves are calculated for the small parameter value $\varepsilon = 0.1$.

corrections up to the post-Newtonian order for the effect of dragging of inertial frames. From this, we found the same time-asymmetric light curves as in the two-point-mass lenses where $l \ll r_E$. Furthermore, we have introduced the cutoff dependent skewness and estimated the asymmetry in the light curves quantitatively. In particular, we showed the clear difference in the skewness for almost similar light curves.

Here we make a comment on the additional factor for the asymmetry in the binary system. In this paper, we have assumed that the lens systems of the two point masses are fixed, but each star constituting the binary revolves around the center of mass. Therefore, the rotational effect may also appear. However, if the rotation period $T \sim (l^3/(G(M_1 + M_2)))^{1/2}$ of the binary is much larger than the typical time scale t_0 of a microlensing event, our consideration of the fixed lens systems would be appropriate. For the extreme case $T \ll t_0$, the time-averaged gravitational potential which is projected on to the lens plane may be regarded approximately as that of a single-point-mass lens or a fixed two-point-mass lens with $l \ll r_E$ if the lens is compact. Therefore, more complicated variations of light curves, corresponding to the phase, are expected only if $T \sim t_0$.

It is very interesting whether the time-asymmetric features of light curves discussed in this paper will actually be detected by the projects (MOA, etc.) that are now in progress.

Acknowledgements

This work was supported in part by a Grant-in-Aid for Scientific Research Fund of the Ministry of Education, Science, Sports and Culture of Japan (08640378).

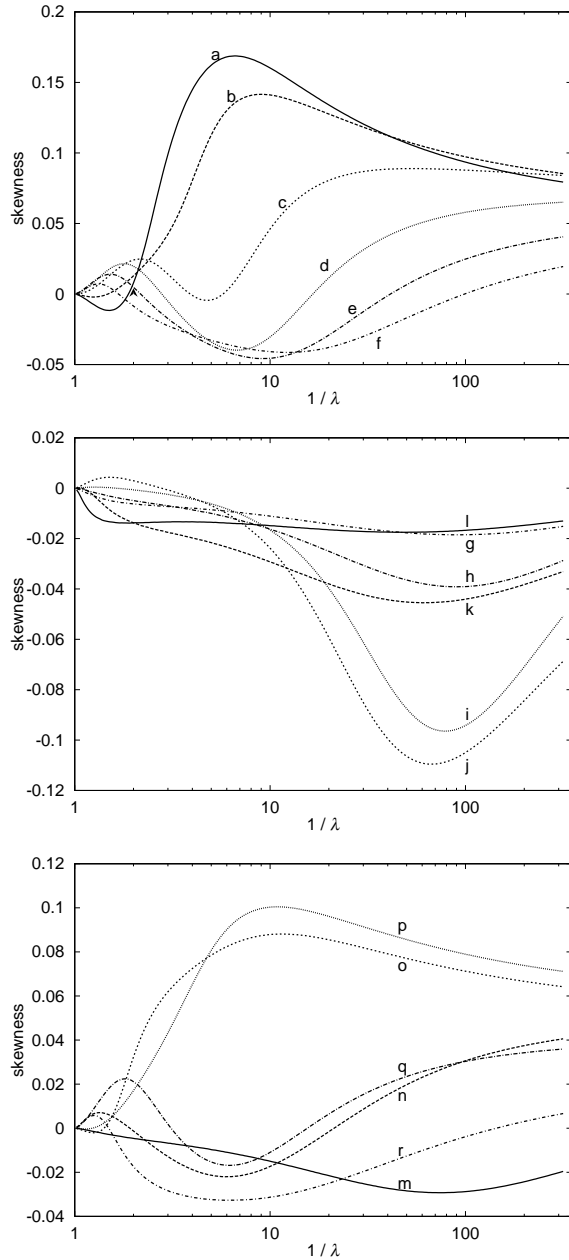


Fig. 10. The skewness of light curves in the planetary system. The curves labeled ‘a’–‘r’ correspond to the points labeled ‘a’–‘r’, respectively, in Fig. 5. The light curves are calculated for the small parameter value $\mu = 0.05$.

References

- [1] See, e.g., B. Paczyński, *Ann. Rev. Astr. Ap.* **34** (1996), 419; R. Narayan and M. Bartelmann, *Lectures on Gravitational Lensing*, preprint: astro-ph/9606001.
- [2] K. Chang and S. Refsdal, *Nature* **282** (1979), 561.
- [3] J. R. Gott, *Astrophys. J.* **243** (1981), 140.

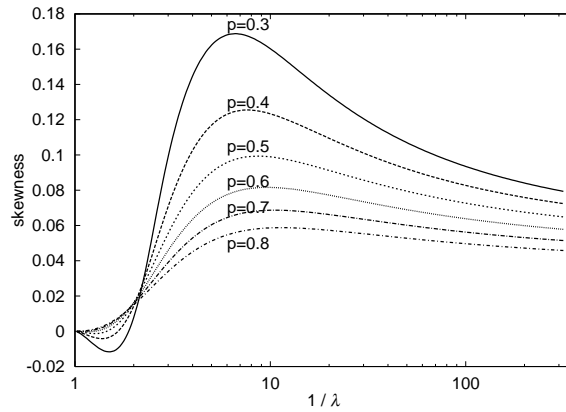


Fig. 11. Dependence of the skewness on the impact parameter p in the planetary case. The light curves correspond to the point ‘a’ in Fig. 5, and are calculated for the small parameter value $\mu = 0.05$.

- [4] A. Gould, *Astrophys. J.* **392** (1992), 442.
- [5] C. Alcock, R. A. Allsman, D. Alves, et al., *Astrophys. J.* **454** (1995), L125.
- [6] B. S. Gaudi and A. Gould, *Astrophys. J.* **482** (1997), 83.
- [7] S. Mao and B. Paczyński, *Astrophys. J.* **374** (1991), L37.
- [8] A. Gould and A. Loeb, *Astrophys. J.* **396** (1992), 104.
- [9] A. D. Bolatto and E. E. Falco, *Astrophys. J.* **436** (1994), 112.
- [10] D. P. Bennett and S. H. Rhie, *Astrophys. J.* **472** (1996), 660.
- [11] B. S. Gaudi and A. Gould, *Astrophys. J.* **486** (1997), 85.
- [12] P. Schneider and A. Weiss, *Astron. Astrophys.* **164** (1986), 237.
- [13] S. O. Sari, *Astrophys. J.* **462** (1996), 110.
- [14] See, e.g., W. H. Press et al., *Numerical Recipes in Fortran* (Cambridge University Press, 1992).